

Compton and Thomson scattering in strong magnetic fields

H. Herold

Institut für Theoretische Physik der Universität Erlangen-Nürnberg, D-8520 Erlangen, Federal Republic of Germany

(Received 10 April 1978; revised manuscript received 1 February 1979)

The differential cross section for scattering of photons by electrons in a strong magnetic field is calculated. The relativistic treatment is performed for electrons in the lowest Landau level. By specializing to the nonrelativistic region, cross sections for Thomson scattering are given for an arbitrary direction of the photon with respect to the magnetic field. These results are in agreement with previous calculations. The relativistic cross sections are numerically calculated to compare them explicitly with the nonrelativistic case and to present numerical values which can be used, for instance, in practical applications to neutron stars.

I. INTRODUCTION

In the strong magnetic fields (10^{12} – 10^{13} G) which are present at the surfaces of neutron stars the interaction of electrons and photons is greatly altered, because the electrons are restricted to moving perpendicular to the field in Landau orbitals. Recent experiments for the binary x-ray source Her X-1 have shown^{1,2} that in this case the distance between the Landau levels is approximately 58 keV. This result leads to a magnetic field of roughly $0.1B_{cr}$, where the critical field is $B_{cr} = m^2/e = 4.414 \times 10^{13}$ G (we use natural units $\hbar = c = 1$ throughout).

In those circumstances the cross section for scattering of photons by electrons (Thomson scattering in the nonrelativistic region) is strongly changed in comparison with the results without magnetic field. This can already be seen by classical calculations in the nonrelativistic case.³⁻⁵ These results have been used to explain the radiation from accreting x-ray pulsars.⁶⁻⁸ If the value of the magnetic field approaches B_{cr} , quantum effects and relativistic corrections become essential so that a relativistic quantum treatment is necessary. This is performed in this paper in order to show the difference with the nonrelativistic results.

Considerable work has been done on quantum-electrodynamic (QED) effects in strong magnetic fields.⁹⁻¹¹ But frequently only the weak-field limit ($B/B_{cr} \ll 1$) is considered. Moreover, many authors deal with the region where the electrons are highly relativistic, a domain in which the discrete structure of the electron levels is negligible. In the situation in which we are interested both conditions are not valid.

As for relativistic Compton scattering in arbitrary high magnetic fields, Hari Dass *et al.* have treated this problem.^{12,13} In this work the authors calculated the cross section under the restriction that the incoming photon propagates parallel to the magnetic field. They stress that it is necessary

to relax this constraint in further work.

We shall do this in the present paper wherein we calculate the Compton scattering in the more general case, in which the directions of the incoming photon and of the magnetic field do not coincide. This task is performed by the conventional approach of summing over intermediate states with the help of the exact electron propagator in a magnetic field, in contrast to the method of Ref. 13 where Schwinger's source theory¹⁴ is used. This calculation is carried out in order to present numerical results explicitly.

As for the applicability to the situation near the surface of a neutron star, it is assumed that the photon frequency is well above the plasma frequency of the electrons. Therefore the photon scattering can be treated as an elementary process between photon and electron, and the influence of plasma effects as discussed for QED processes by Melrose¹⁵ can be neglected.

II. CROSS SECTION FOR COMPTON SCATTERING IN A STRONG MAGNETIC FIELD

The process we will describe is characterized by

- (a) a magnetic field in the z direction, $\vec{B} = B\vec{e}_z$,
- (b) an incoming photon with momentum \vec{k} and polarization vector \vec{e}_s ($s = 1, 2$),
- (c) an electron in the lowest Landau level $N = 0$ with momentum $p_z = 0$,
- (d) a scattered photon with momentum \vec{k}' and polarization vector $\vec{e}_{s'}$,
- (e) a recoiled electron also in the lowest Landau level $N' = 0$ with momentum p'_z .

The assumption $p_z = 0$ for the initial state of the electron is no restriction, since the results for $p_z \neq 0$ are easily determined by a Lorentz transformation in the z direction. The assumption $N' = 0$ for the final state of the electron is fully correct if the photon frequency ω is less than the cyclotron frequency $\omega_B = eB/m$, otherwise the excitation of the electron into higher Landau levels may

additionally be taken into account (which corresponds to Raman scattering).

We use the Landau gauge for the vector potential of the magnetic field: $\vec{A} = Bx\vec{e}_y$. Thus, for completeness, we will give the well-known solutions of the Dirac equation in a homogeneous magnetic field¹⁶ that will be used in the following ($N = 0, 1, 2, \dots$):

(a) positive-energy eigenstates (electrons)

$$u_{Np_z p_y h}(\vec{x}, t) = \begin{pmatrix} \left(\frac{\epsilon + m}{2\epsilon}\right)^{1/2} \\ \hbar \left(\frac{\epsilon - m}{2\epsilon}\right)^{1/2} \end{pmatrix} w_{Np_z p_y h}(\vec{x}) e^{-i\epsilon t}; \quad (1a)$$

(b) negative-energy eigenstates (positrons)

$$v_{Np_z p_y h}(\vec{x}, t) = \begin{pmatrix} -\hbar \left(\frac{\epsilon - m}{2\epsilon}\right)^{1/2} \\ \left(\frac{\epsilon + m}{2\epsilon}\right)^{1/2} \end{pmatrix} w_{N-p_z -p_y h}(\vec{x}) e^{i\epsilon t}. \quad (1b)$$

with the spinors

$$w_{Np_z p_y h}(\vec{x}) = \frac{1}{\sqrt{2}} \left\{ [1 - \hbar p_z (\epsilon^2 - m^2)^{-1/2}]^{1/2} w_{Np_z p_y}^{(-)} - i\hbar [1 + \hbar p_z (\epsilon^2 - m^2)^{-1/2}]^{1/2} w_{Np_z p_y}^{(+)} \right\} \quad (2)$$

$$S_{fi} = (-ie)^2 \int_{-\infty}^{\infty} dt \int_{-\infty}^{\infty} dt' \int d^3x d^3x' (2V\omega)^{-1/2} (2V\omega')^{-1/2} \times \sum_{i,j} \left\{ u_{\lambda'}^{\dagger}(\vec{x}, t) \alpha_i \left[\sum_{\lambda''} u_{\lambda''}(\vec{x}, t) u_{\lambda''}^{\dagger}(\vec{x}', t') \theta(t-t') - \sum_{\lambda''} v_{\lambda''}(\vec{x}, t) v_{\lambda''}^{\dagger}(\vec{x}', t') \theta(t'-t) \right] \times \alpha_j u_{\lambda}(\vec{x}', t') \left(e_{s_i} e^{i(\vec{k} \cdot \vec{x} - \omega t)} e_{s'_j}^* e^{-i(\vec{k}' \cdot \vec{x}' - \omega' t')} + e_{s'_j} e^{-i(\vec{k}' \cdot \vec{x}' - \omega' t')} e_{s_i} e^{i(\vec{k} \cdot \vec{x} - \omega t)} \right) \right\}. \quad (5)$$

In terms of Feynman diagrams we have the well-known graphs, shown in Fig. 1, corresponding to the two photon terms in the above expression. The sum in square brackets in (5) is the relativistic electron propagator in the magnetic field, i.e., the positive-energy electron propagates "forward in time," the negative-energy electron "backward in time."

The kinematic restrictions following from (5) are momentum conservation in the z direction and energy conservation, i.e.,

$$p_z + k_z = p'_z + k'_z, \quad (6)$$

$$\omega + (m^2 + p_z^2 + 2NeB)^{1/2} = \omega' + (m^2 + p_z'^2 + 2N'eB)^{1/2}.$$

We denote the angle between the incoming (outgoing) photon and the magnetic field by θ (θ'). Thus, for $N = N' = 0$, the energy of the scattered photon, determined from (6), is given by

$$\omega' = \{m + \omega(1 - \cos\theta \cos\theta') - [m^2 + 2m\omega \cos\theta'(\cos\theta' - \cos\theta) + \omega^2(\cos\theta' - \cos\theta)^2]^{1/2}\} / \sin^2\theta'. \quad (7)$$

This replaces the well-known Compton formula without magnetic field where the electron motion is not restricted to "one dimension."

Inserting the wave functions (1) into the S matrix (5), the differential cross section is obtained by a straightforward but lengthy calculation. In this task the paper of Canuto and Ventura¹⁷ has been found to be

and the abbreviation

$$w_{Np_z p_y}^{(\tau)} = (L_x L_y)^{-1/2} e^{ip_z z} e^{ip_y y} \times \varphi_n((eB)^{1/2}(x + p_y/eB))(eB)^{1/4} |\tau\rangle_{\text{spin}} \quad (3)$$

$$[n = N - (1 + \tau)/2, \quad \tau = \pm 1],$$

where $\varphi_n(\xi)$ are the normalized eigenfunctions of the one-dimensional harmonic oscillator. The energies ϵ are given by $\epsilon(N, p_z) = (m^2 + p_z^2 + 2NeB)^{1/2}$.

Besides the p_y degeneracy [number of p_y values = $(eB/2\pi)L_x L_y$], the $N > 0$ levels are double and differ by the helicity $h = \pm 1$ [eigenvalue of the operator $\vec{\sigma} \cdot (\vec{\beta} - e\vec{A})/(\epsilon^2 - m^2)^{1/2}$]. The $N = 0$ level has only possibility for h , namely $h = -p_z/|p_z|$ or $\tau = -1$.

The S matrix for Compton scattering (as a second-order process) can be written as

$$S^{(2)} = (-i)^2 \int_{-\infty}^{\infty} dt \int_{-\infty}^t dt' H_I(t) H_I(t')$$

with

$$H_I(t) = e \int d^3x : \Psi^{\dagger}(\vec{x}, t) \vec{\alpha} \Psi(\vec{x}, t) : \vec{A}^{\text{ph}}(\vec{x}, t), \quad (4)$$

where $\Psi(\vec{x}, t)$ is the (second-quantized) electron field and $\vec{A}^{\text{ph}}(\vec{x}, t)$ is the photon field.

Inserting the initial and final states $|\lambda\rangle_e |\vec{k}, s\rangle_{\text{ph}}$ and $|\lambda'\rangle_e |\vec{k}', s'\rangle_{\text{ph}}$, we obtain the matrix element

very useful. We omit the details, but mention only that in the time integration the step functions $\theta(t-t')$ are replaced by well-known integral representations (in this way, energy denominators appear). Moreover, it must be averaged over the p_y degeneracy of the initial electron level.

Finally, this calculation results in the following formula for the differential cross section, where $d\Omega'$ is the solid angle of the scattered photon (the recoiled electron is not observed):

$$\frac{d\sigma}{d\Omega'} = \frac{1}{2} \alpha^2 \frac{\omega'}{\omega} (2m + \omega - \omega')^{-1} [m + \omega - \omega' - (k_z - k'_z) \cos\theta']^{-1} \exp\left(-\frac{k_\perp^2 + k'_\perp^2}{2eB}\right) \left| \sum_{N''=0}^{\infty} [a_1(N'', s - s') + a_2(N'', s - s')] \right|^2 \quad (8)$$

with

$$a_1(N'', s - s') = \frac{1}{2m\omega' - k'_\perp{}^2 + 2N''eB} \left[\frac{1}{N''!} \left(\frac{k_\perp k'_\perp}{2eB}\right)^{N''} e^{iN''(\varphi - \varphi')} [\omega'(2m + \omega - \omega') + k'_z(k_z - k'_z)] e_{sz} e_{s'_z}^* + \frac{1}{(N'' - 1)!} \left(\frac{k_\perp k'_\perp}{2eB}\right)^{N''-1} e^{i(N''-1)(\varphi - \varphi')} \{ [\omega'(2m + \omega - \omega') - k'_z(k_z - k'_z)] \times (e_{sx} + ie_{sy})(e_{s'_x}^* - ie_{s'_y}^*) + (k_z - k'_z)(k_x + ik_y) e_{sz} (e_{s'_x}^* - ie_{s'_y}^*) + (k_z - k'_z)(k'_x - ik'_y) e_{s'_z}^* (e_{sx} + ie_{sy}) \} \right] \quad (9a)$$

and

$$a_2(N'', s - s') = \frac{1}{2m\omega + k_\perp^2 - 2N''eB} \left[\frac{1}{N''!} \left(\frac{k_\perp k'_\perp}{2eB}\right)^{N''} e^{-iN''(\varphi - \varphi')} [\omega(2m + \omega - \omega') + k_z(k_z - k'_z)] e_{sz} e_{s'_z}^* + \frac{1}{(N'' - 1)!} \left(\frac{k_\perp k'_\perp}{2eB}\right)^{N''-1} e^{-i(N''-1)(\varphi - \varphi')} \times \{ [\omega(2m + \omega - \omega') - k_z(k_z - k'_z)] (e_{sx} - ie_{sy})(e_{s'_x}^* + ie_{s'_y}^*) + (k_z - k'_z)(k_x - ik_y) e_{sz} (e_{s'_x}^* + ie_{s'_y}^*) + (k_z - k'_z)(k'_x + ik'_y) e_{s'_z}^* (e_{sx} - ie_{sy}) \} \right] \times \exp\left(i \frac{k_\perp k'_\perp}{eB} \sin(\varphi - \varphi')\right). \quad (9b)$$

In this formula, N'' characterizes the Landau levels of the electron intermediate states. We have not tried to sum up over N'' (this would yield confluent hypergeometric functions), because the convergence of this sum is very fast, which makes the unavoidable numerical calculation quite easy. The abbreviations k_\perp and k'_\perp in (8) and (9) mean the photon momenta orthogonal to the magnetic field: $k_\perp = \omega \sin\theta$, $k'_\perp = \omega' \sin\theta'$.

III. DISCUSSION AND RESULTS

Before we present numerical results we want to describe some properties and limiting cases of the general formula (8).

The photon scattering shows resonances where the denominator in the amplitude (9b), corresponding to the second diagram of Fig. 1, vanishes:

$$2m\omega + \omega^2 \sin^2\theta - 2N''eB = 0.$$

This leads to the resonance energies

$$\omega_{\text{res}}^{(N'')}(\theta) = [(m^2 + 2N''eB \sin^2\theta)^{1/2} - m] / \sin^2\theta. \quad (10)$$

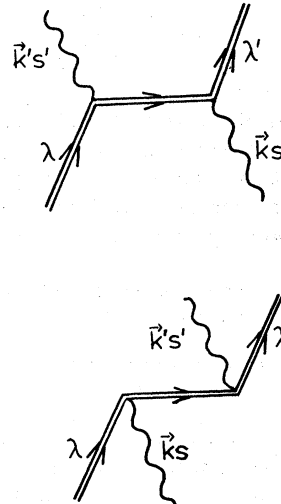


FIG. 1. Diagrams for Compton scattering in a magnetic field. The double line indicates electron propagation in the uniform magnetic field.

For $\theta=0$ (photon parallel to the magnetic field), these are multiples of the cyclotron frequency ω_B :

$$\omega_{\text{res}}^{(N)}(\theta=0) = NeB/m = N\omega_B. \quad (11)$$

Generally, the resonance energies are smaller. This can be seen by the expansion for $B/B_{\text{cr}} \ll 1$,

$$\omega_{\text{res}}^{(N)}(\theta) = N\omega_B [1 - N(B/B_{\text{cr}}) \sin^2\theta + \dots], \quad (12)$$

and additionally by Table I which gives the first resonance energies for two values of the magnetic field and for three angles $\theta \neq 0$.

Nonrelativistically, there is only one resonance, the well-known cyclotron resonance at $\omega = \omega_B$. This can be shown if we specialize formula (8) to the nonrelativistic case which means

$$\omega/m \ll 1, \quad B/B_{\text{cr}} = eB/m^2 = \omega_B/m \ll 1. \quad (13)$$

In this case, the general formula greatly simplifies (from the sum over N'' only the $N''=0$ and $N''=1$ terms remain) and we obtain ($r_0 = \alpha/m$)

$$\frac{d\sigma}{d\Omega'} = \frac{1}{4} r_0^2 |a(s - s')|^2 \quad (14)$$

with

$$\begin{aligned} a(1-1) &= 2 \sin\theta \sin\theta' + \cos\theta \cos\theta' \\ &\times \left(e^{i(\varphi-\varphi')} \frac{\omega}{\omega+\omega_B} + e^{-i(\varphi-\varphi')} \frac{\omega}{\omega-\omega_B} \right), \\ a(2-2) &= e^{i(\varphi-\varphi')} \frac{\omega}{\omega+\omega_B} + e^{-i(\varphi-\varphi')} \frac{\omega}{\omega-\omega_B}, \\ a \begin{pmatrix} 1-2 \\ 2-1 \end{pmatrix} &= \begin{pmatrix} -i \cos\theta \\ i \cos\theta' \end{pmatrix} \\ &\times \left(e^{i(\varphi-\varphi')} \frac{\omega}{\omega+\omega_B} - e^{-i(\varphi-\varphi')} \frac{\omega}{\omega-\omega_B} \right). \end{aligned} \quad (15)$$

Here we indicate by 1 the linear polarization of the photon parallel to the plane built up by the magnetic field and the incoming photon, and by 2 the linear polarization orthogonal to this plane.

The total cross section, obtained by integrating over Ω' and summing over the scattered photon

TABLE I. Cyclotron resonance energies $\omega_{\text{res}}^{(N)}(\theta)$ in units of ω_B for two values of B : (1) $B/B_{\text{cr}} = 1.0$, (2) $B/B_{\text{cr}} = 0.1$.

N	$\theta = 30^\circ$		$\theta = 60^\circ$		$\theta = 90^\circ$	
	(2)	(1)	(2)	(1)	(2)	(1)
1	0.9878	0.8990	0.9651	0.7749	0.9545	0.7321
2	1.9524	1.6569	1.8690	1.3333	1.8322	1.2361
3	2.8952	2.3246	2.7221	1.7936	2.6491	1.6458
4	3.8178	2.9282	3.5321	2.1943	3.4164	2.0000
5	4.7214	3.4833	4.3050	2.5540	4.1421	2.3166

polarizations, is given by $[\sigma_{\text{Th}} = (8\pi/3)r_0^2]$

$$\begin{aligned} \sigma_{\text{tot}}(1) &= \sigma_{\text{Th}} \left\{ \sin^2\theta + \frac{1}{2} \cos^2\theta \left[\frac{\omega^2}{(\omega+\omega_B)^2} + \frac{\omega^2}{(\omega-\omega_B)^2} \right] \right\}, \\ \sigma_{\text{tot}}(2) &= \sigma_{\text{Th}} \frac{1}{2} \left[\frac{\omega^2}{(\omega+\omega_B)^2} + \frac{\omega^2}{(\omega-\omega_B)^2} \right]. \end{aligned} \quad (16)$$

In an analogous way the results for circular polarization (\pm) may be calculated. This leads to

$$\begin{aligned} \sigma_{\text{tot}}(\pm) &= \sigma_{\text{Th}} \left\{ \frac{1}{2} \sin^2\theta + \frac{1}{4} (1 + \cos^2\theta) \right. \\ &\times \left[\frac{\omega^2}{(\omega+\omega_B)^2} + \frac{\omega^2}{(\omega-\omega_B)^2} \right] \\ &\left. \mp \frac{1}{2} \cos\theta \left[\frac{\omega^2}{(\omega+\omega_B)^2} - \frac{\omega^2}{(\omega-\omega_B)^2} \right] \right\}. \end{aligned} \quad (17)$$

It is seen that, nonrelativistically, there is only the resonance at $\omega = \omega_B$. The reason for this is the well-known fact that in the oscillator only neighboring levels are coupled by the momentum or position operator. This feature vanishes in the relativistic treatment.

The nonrelativistic formulas (16) and (17) are in agreement with the results of the classical calculation of magnetic Thomson scattering.³ They show a strong dependence of the scattering cross section on the direction of the incoming photon. For instance, for $\theta=0$ and $\omega \ll \omega_B$ the cross section is strongly reduced in comparison with the Thomson value ($\sigma_{\text{tot}} \approx \sigma_{\text{Th}} \omega^2 / \omega_B^2$), but for $\theta \neq 0$ this property disappears, at least for polarization 1. For $\theta = \pi/2$ the cyclotron resonance is completely suppressed for polarization 1.¹⁸

In order to discuss the general formula, we calculated the cross section numerically. For this purpose we have written a FORTRAN program

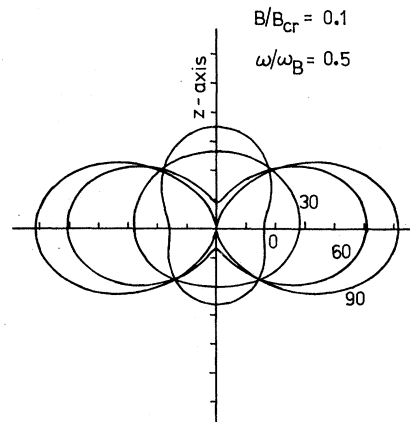


FIG. 2. Polar diagram of $\int (d\sigma/d\Omega') d\varphi'$, given in units of r_0^2 , for photon polarization 1 (parallel to incoming plane). The various incoming angles θ are given in degrees at the distinct curves.

TABLE II. Total cross section σ_{tot} in units of r_0^2 as a function of ω/ω_B , in the nonrelativistic limit ($nr, B/B_{\text{cr}} \ll 1$) and for two values of B : (1) $B/B_{\text{cr}} = 1.0$, (2) $B/B_{\text{cr}} = 0.1$.

(a)						
$\theta = 0^\circ$						
ω/ω_B	nr	circ. polar. +		nr	circ. polar. -	
		(2)	(1)		(2)	(1)
0.1	0.1034	0.1014	0.0861	0.0692	0.0680	0.0585
0.2	0.5236	0.5029	0.3723	0.2327	0.2250	0.1735
0.3	1.539	1.448	0.9520	0.4461	0.4254	0.3010
0.4	3.723	3.433	2.032	0.6839	0.6440	0.4245
0.5	8.378	7.565	4.074	0.9308	0.8666	0.5372
0.6	18.85	16.67	8.235	1.178	1.085	0.6372
0.7	45.61	39.50	18.02	1.420	1.295	0.7239
0.8	134.0	113.6	48.17	1.655	1.494	0.7979
0.9	678.6	563.2	222.8	1.880	1.680	0.8601
1.0	res.	res.	res.	2.094	1.854	0.9116
1.1	1014.0	805.8	281.0	2.299	2.015	0.9535
1.2	301.6	234.6	77.17	2.493	2.164	0.9868
1.3	157.3	119.7	37.25	2.676	2.301	1.012
1.4	102.6	76.39	22.55	2.851	2.426	1.031
1.5	75.40	54.89	15.40	3.016	2.541	1.044
1.6	59.57	42.42	11.33	3.173	2.646	1.052
1.7	49.41	34.40	8.772	3.321	2.742	1.055
1.8	42.41	28.87	7.037	3.462	2.828	1.055
1.9	37.34	24.84	5.799	3.596	2.906	1.051
2.0	33.51	21.80	4.879	3.723	2.976	1.044
2.1	30.53	19.41	4.173	3.844	3.039	1.034
2.2	28.16	17.49	3.617	3.960	3.095	1.022
2.3	26.22	15.92	3.169	4.070	3.144	1.009
2.4	24.62	14.60	2.803	4.174	3.188	0.9941

(b)						
$\theta = 30^\circ$						
ω/ω_B	nr	lin. polar. 1		nr	lin. polar. 2	
		(2)	(1)		(2)	(1)
0.1	2.159	2.154	2.120	0.0863	0.0850	0.0748
0.2	2.378	2.359	2.237	0.3782	0.3667	0.2912
0.3	2.839	2.783	2.474	0.9924	0.9480	0.6918
0.4	3.747	3.609	2.924	2.204	2.075	1.418
0.5	5.585	5.262	3.842	4.654	4.325	2.843
0.6	9.605	8.859	6.004	10.01	9.217	6.115
0.7	19.73	17.98	12.69	23.52	21.61	16.06
0.8	52.98	48.86	51.71	67.85	63.62	73.60
0.9	257.3	264.1	52 544	340.2	356.6	771 740
1.0	res.	16 312	60.92	res.	22 238	86.73
1.1	383.1	230.0	18.02	508.0	311.5	23.96
1.2	116.1	76.42	9.573	152.0	101.9	11.70
1.3	62.09	41.67	6.549	79.99	54.51	7.389
1.4	41.65	27.99	5.398	52.74	35.85	5.829
1.5	31.50	21.06	6.185	39.21	26.41	7.146
1.6	25.62	17.01	26.30	31.37	20.91	37.16
1.7	21.87	14.50	52.69	26.37	17.52	75.48
1.8	19.30	13.30	8.008	22.94	15.93	9.886
1.9	17.44	21.27	4.549	20.47	27.05	4.921
2.0	16.06	26.19	3.472	18.62	33.95	3.440
2.1	14.99	11.33	3.090	17.19	13.39	2.976
2.2	14.14	9.461	3.752	16.06	10.85	4.052
2.3	13.45	8.541	47.33	15.15	9.629	68.15
2.4	12.89	7.904	8.133	14.40	8.799	10.39

TABLE II. (Continued).

(c)						
$\theta = 60^\circ$						
ω/ω_B	lin. polar. 1			lin. polar. 2		
	nr	(2)	(1)	nr	(2)	(1)
0.1	6.305	6.276	6.053	0.0863	0.0856	0.0799
0.2	6.378	6.310	5.832	0.3782	0.3722	0.3300
0.3	6.531	6.410	5.639	0.9924	0.9707	0.8362
0.4	6.834	6.640	5.532	2.204	2.149	1.872
0.5	7.447	7.154	5.702	4.654	4.551	4.344
0.6	8.787	8.370	7.085	10.01	9.939	12.55
0.7	12.16	11.71	21.11	23.52	24.32	76.85
0.8	23.25	24.44	187.6	67.85	78.48	745.1
0.9	91.34	151.6	12.83	340.2	617.6	32.56
1.0	res.	611.2	6.924	res.	2574.0	11.03
1.1	133.3	53.36	5.344	508.0	203.9	6.414
1.2	44.29	23.79	5.180	152.0	78.47	7.307
1.3	26.28	15.73	25.14	79.99	44.55	82.60
1.4	19.47	12.26	11.58	52.74	30.21	26.61
1.5	16.08	10.39	5.053	39.21	22.73	6.312
1.6	14.13	9.283	4.031	31.37	18.51	3.879
1.7	12.87	8.797	4.283	26.37	16.98	5.696
1.8	12.02	11.61	332.2	22.94	29.92	984.8
1.9	11.40	32.94	5.094	20.47	124.3	6.048
2.0	10.94	8.672	3.978	18.62	18.15	2.970
2.1	10.58	7.219	4.389	17.19	12.32	3.596
2.2	10.30	6.614	261.1	16.06	10.22	678.5
2.3	10.07	6.214	pos.	15.15	9.004	3.872
2.4	9.882	5.901	pos.	14.40	8.168	2.229

(d)						
$\theta = 90^\circ$						
ω/ω_B	lin. polar. 1			lin. polar. 2		
	nr	(2)	(1)	nr	(2)	(1)
0.1	8.378	8.329	7.943	0.0863	0.0859	0.0826
0.2	8.378	8.266	7.478	0.3782	0.3749	0.3505
0.3	8.378	8.191	6.990	0.9924	0.9822	0.9160
0.4	8.378	8.102	6.490	2.204	2.186	2.144
0.5	8.378	8.001	6.022	4.654	4.668	5.408
0.6	8.378	7.890	5.954	10.01	10.32	19.23
0.7	8.378	7.777	25.66	23.52	25.83	360.7
0.8	8.378	7.714	14.03	67.85	87.66	86.76
0.9	8.378	8.886	6.869	340.2	861.8	15.39
1.0	8.378	11.03	5.449	res.	1477.0	7.079
1.1	8.378	7.791	4.846	508.0	170.8	6.716
1.2	8.378	7.354	10.81	152.0	69.91	60.73
1.3	8.378	7.101	8.724	79.99	40.68	24.90
1.4	8.378	6.891	4.920	52.74	27.96	5.780
1.5	8.378	6.696	4.218	39.21	21.29	3.985
1.6	8.378	6.509	5.819	31.37	17.76	16.51
1.7	8.378	6.340	7.976	26.37	18.39	15.35
1.8	8.378	6.795	5.311	22.94	114.5	3.647
1.9	8.378	6.205	6.960	20.47	40.90	3.373
2.0	8.378	5.836	pos.	18.62	15.70	res.
2.1	8.378	5.629	pos.	17.19	11.55	3.948
2.2	8.378	5.443	pos.	16.06	9.717	2.452
2.3	8.378	5.264	pos.	15.15	8.596	42.69
2.4	8.378	5.091	pos.	14.40	7.839	3.570

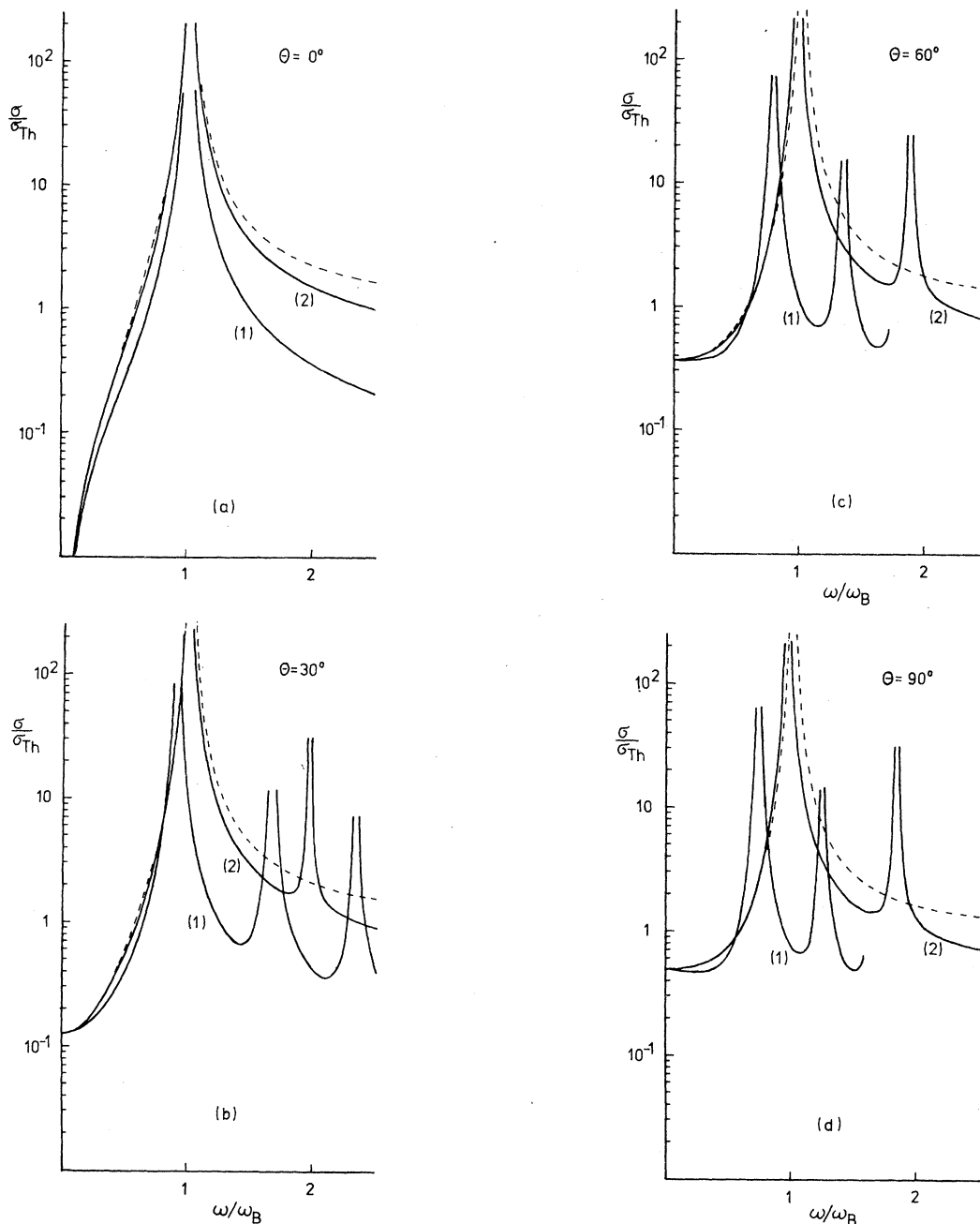


FIG. 3. Total cross sections (unpolarized) in units of σ_{Th} vs frequency ω in units of ω_B , for two values of B : (1) $B/B_{cr} = 1.0$, (2) $B/B_{cr} = 0.1$. The dashed line is the nonrelativistic limit (Thomson limit). The angle θ varies from (a) to (d) as indicated.

which computes the differential cross section (8) for arbitrary photon polarizations and the other input parameters. The cross section integrated by φ' or by φ' and θ' is also calculated. As an example, we give in Fig. 2 some θ' -angular distributions for different values of θ with fixed photon energy.

As for the total cross section, we decided to pre-

sent it as a function of the photon energy for two values of B and for the angles $\theta = 0^\circ, 30^\circ, 60^\circ, 90^\circ$. This is done in Table II where, for comparison, the nonrelativistic limit is also shown. For $\theta = 0$ the photon is assumed to be circularly polarized (the natural choice), while for $\theta \neq 0$ the photon is linearly polarized, parallel or orthogonal, to the incoming plane. This choice is suggested by the

fact that the vacuum polarization in strong magnetic fields leads to photon propagation in these linearly polarized modes.^{9,19,20} Moreover, the magnitude of this photon energy splitting¹⁹⁻²¹ shows²² that the plasma effects (for the usual plasma densities) which would produce elliptic polarization cannot disturb the linear polarization; only in the proximity of $\theta = 0^\circ$ do the polarization modes change from linear to circular, depending on the plasma density.

As already mentioned, the cyclotron resonance is related to the energy denominator of (9b). If, on the other hand, the denominator in (9a) vanishes, this means that in the intermediate state of the first diagram of Fig. 1 the virtual electron becomes real as a positron (pair creation in the magnetic field⁹). This effect occurs if the photon energy ω is greater than $2m/\sin\theta$. Above this thresh-

hold the cross section (for polarization 1) can no longer be calculated by (9). This is indicated in Table II by "pos."

Additionally, in Fig. 3(a)-3(d) the total cross section for unpolarized photons is given together with the nonrelativistic limit. With respect to this case, the appearance of the higher cyclotron resonances is an outstanding feature of the relativistic treatment. This property disappears only for $\theta = 0$, because the $N'' > 1$ terms in (9) are not present for $k_\perp = 0$. Moreover, the fact that for $\theta \neq 0$ the resonance energies are shifted to lower frequencies is evident in particular for higher values of the magnetic field and large angles θ .

ACKNOWLEDGMENT

The author would like to thank Professor H. Ruder for valuable suggestions and helpful discussions.

¹J. Trümper, W. Pietsch, C. Reppin, B. Sacco, E. Kendziorra, and R. Staubert, *Ann. N. Y. Acad. Sci.* **302**, 538 (1977).

²J. Trümper, W. Pietsch, C. Reppin, W. Voges, R. Staubert, and E. Kendziorra, *Astrophys. J.* **219**, L105 (1978).

³V. Canuto, J. Lodenquai, and M. Ruderman, *Phys. Rev. D* **3**, 2303 (1971).

⁴Yu. N. Gnedin and R. A. Sunyaev, *Zh. Eksp. Teor. Fiz.* **65**, 102 (1973) [*Sov. Phys.—JETP* **38**, 51 (1974)].

⁵G. Börner and P. Meszaros, *Plasma Phys.* (to be published).

⁶Yu. N. Gnedin and R. A. Sunyaev, *Astron. Astrophys.* **36**, 379 (1974).

⁷M. M. Basko and R. A. Sunyaev, *Astron. Astrophys.* **42**, 311 (1975).

⁸P. Meszaros, *Astron. Astrophys.* **63**, L19 (1978).

⁹J. S. Toll, Ph.D. thesis, Princeton Univ., 1952 (unpublished).

¹⁰T. Erber, *Rev. Mod. Phys.* **38**, 626 (1966).

¹¹P. Urban, *Ann. N. Y. Acad. Sci.* **257**, 16 (1975), and further references cited therein.

¹²N. D. Hari Dass, L. L. DeRaad, Jr., K. A. Milton, and W.-Y. Tsai, *Ann. N. Y. Acad. Sci.* **257**, 72 (1975).

¹³K. A. Milton, W.-Y. Tsai, L. L. DeRaad, Jr., and N. D. Hari Dass, *Phys. Rev. D* **10**, 1299 (1974).

¹⁴J. Schwinger, *Particles, Sources and Fields* (Addison-Wesley, Reading, Mass., 1970).

¹⁵D. B. Melrose, *Plasma Phys.* **16**, 845 (1974).

¹⁶M. H. Johnson and B. A. Lippmann, *Phys. Rev.* **76**, 828 (1949).

¹⁷V. Canuto and J. Ventura, *Fund. Cosmic Phys.* **2**, 203 (1977).

¹⁸A broader discussion of the properties of Thomson scattering is given by J. Ventura, *Phys. Rev. D* **19**, 1684 (1979).

¹⁹S. L. Adler, *Ann. Phys. (N.Y.)* **67**, 599 (1971).

²⁰D. B. Melrose and R. J. Stoneham, *J. Phys. A* **10**, 1211 (1977).

²¹W.-Y. Tsai and T. Erber, *Phys. Rev. D* **10**, 492 (1974); **12**, 1132 (1975).

²²P. Meszaros and J. Ventura, *Phys. Rev. Lett.* **41**, 1544 (1978).